Environ Chem Lett (2017) 15:467–474
DOI 10.1007/s10311-017-0610-x

ORIGINAL PAPER

High reduction of 4-nitrophenol using reduced graphene oxide/Ag synthesized with tyrosine

Sireesh Babu Maddinedi[1,2] · Badal Kumar Mandal[2] · Nawaz Khan Fazlur-Rahman[3]

Received: 22 August 2016 / Accepted: 9 February 2017 / Published online: 21 February 2017
© Springer International Publishing Switzerland 2017

Abstract There is a demand for the development of environmental friendly methods for the synthesis of graphene composites. Reduced graphene oxide/silver (RGO/Ag) nanocomposites are very good catalysts. Here, we propose a simple, green method for the synthesis of RGO/Ag nanocomposite using the amino acid tyrosine as bioreductant and stabilizing agent. RGO/Ag nanocomposite was characterized by using various analytical techniques and studied for its catalytic degradation of 4-nitrophenol. Results of attenuated total reflectance Fourier transform infrared spectroscopy and Zeta potential at −55 mV reveal the surface capping of tyrosine onto the reduced graphene oxide nanosheets. RGO/Ag nanocomposites show excellent catalytic reduction of 4-nitrophenol with $NaBH_4$, when compared to actual individual silver nanoparticles.

Keywords Graphene oxide · Tyrosine · Silver nanoparticles · Nitrophenol

✉ Badal Kumar Mandal
badalmandal@vit.ac.in

[1] The Key laboratory of Advanced Textile Materials and Manufacturing Technology of Ministry of Education, National Engineering Lab for Textile Fiber Materials and Processing Technology (Zhejiang), College of Materials and Textiles, Zhejiang Sci-Tech University, Hangzhou 310018, China

[2] Trace Elements Speciation Research Laboratory, Department of Chemistry, School of Advanced Sciences, VIT University, Vellore 632014, India

[3] Organic and Medicinal Chemistry Research Laboratory, Organic Chemistry Division, School of Advanced Sciences, VIT University, Vellore, Tamil Nadu 632 014, India

Introduction

Functionalized graphene materials have been studied in the perspective of different applications, such as sensors, field-effect transistors, polymer composites, energy materials and in biological applications, because of their outstanding thermal, mechanical and electrical properties (Akhavan and Ghaderi 2012; Geim and Novoselov 2007). Normally, functionalized graphene oxide can be prepared either by reduction or through the chemical functionalization. Among these, the reduction of graphene oxide is of the greatest significance due to the similarities in properties between the pristine graphene and the reduced graphene oxide. Hence, the production of reduced graphene oxide via the chemical reduction of graphene oxide is the most desirable method for its large-scale synthesis. However, the toxic nature of chemicals such as hydrazine (Stankovich et al. 2007), hydroquinone (Wang et al. 2008) and $NaBH_4$ (Si et al. 2008) makes the chemical reduction less suitable for bio-applications. Therefore, it is essential to find a green and efficient bioreductant for the reduction of graphene oxide.

Eco-friendly bioreductants such as ascorbic acid, green plant extracts and glucose have been used to synthesize reduced graphene oxide (Paredes et al. 2011). Similarly, few green methods have been reported so far for the synthesis of graphene and its composites (Maddinedi and Mandal 2014, 2015; Maddinedi et al. 2017). The main advantage of green reducing agents involves the reduction and subsequent surface functionalization of the synthesized reduced graphene oxide with the biomolecules used. For instance, our groups have reported the use of casein as reducing and stabilizing agent for the reduced graphene oxide synthesis (Maddinedi et al. 2014).

Similarly, we propose a simple process to synthesize reduced graphene oxide nanosheets that involve tyrosine as green reducing and stabilizing agents. Tyrosine is an amino acid which contains a hydroxyl group. The hydroxyl group is oxidized to form its quinine form during the reduction of graphene oxide. We have also prepared reduced graphene oxide/silver composite by taking the advantage of aqueous dispersibility of reduced graphene oxide prepared and the catalytic activity of composite been tested for the reduction of 4-nitrophenol.

Experimental section

Materials

Graphite powder (100 mesh, 99.9995%), hydrogen peroxide (H_2O_2, 30%) and sodium nitrate ($NaNO_3$) were purchased from Sigma–Aldrich Ltd, Bangalore. Potassium permanganate ($KMnO_4$) and all other solvents were purchased from Sd fine Chemicals, Mumbai.

Reduced graphene oxide

Graphene oxide was prepared from natural graphite powder by following modified Hummers method (Perera et al. 2012). To the 50 mL of graphene oxide (1 mg mL^{-1}) dispersion, 500 mg of tyrosine was added and the subsequent mixture was maintained a pH 12 using NH_4OH. The reaction mixture was refluxed at 100 °C on a water bath for about 8 h. The resultant black reduced graphene oxide was centrifuged followed by several times washing with the double-distilled water and ethanol to obtain pure material.

Tyrosine reduced graphene oxide/silver composite

Reduced graphene oxide dispersion was obtained by sonicating the 10 mg of prepared tyrosine reduced graphene oxide material in double-distilled water for about 1 h. To the above dispersion, 10 mL of $AgNO_3$ (1 mM) was added followed by the addition of 2 mL of tyrosine solution (1 mM). The resultant mixture was further sonicated for about 10 min under heating at 60 °C to obtain tyrosine-reduced graphene oxide (TRGO/Ag) composite.

Catalytic activity

To check the catalytic activity of the synthesized TRGO/Ag for the reduction of 4-nitrophenol, a suitable quantity of TRGO/Ag was added to the aqueous mixture of 4-nitrophenol and $NaBH_4$ at room temperature. The gradual disappearance of the bright yellow color of the solution mixture represents the 4-nitrophenol reduction. The variation in the absorbance of 4-nitrophenol at a wavelength of 400 nm was spectrophotometrically monitored with time.

Characterization

UV–visible measurements

UV–visible absorption spectral measurements were recorded using a Jasco UV–visible 950 spectrophotometer. The spectra were recorded at wavelength range between 200 and 800 nm, using double-distilled water for blank measurements.

X-ray photoelectron spectroscopy

X-ray photoelectron spectroscopy analysis was carried out by using a PHI Quantera SXM, scanning X-ray microprobe (ULVac-PHI Inc) instrument. Dried tyrosine reduced graphene oxide and TRGO/Ag powders are homogeneously spread over the surface of silicon wafer separately and pasted on the copper tape, and measurements were performed.

X-ray diffraction

X-ray diffraction analysis of tyrosine reduced graphene oxide was carried out by using a Bruker D8 Advance diffractometer at room temperature with a scanning speed of 4°/min, Cu Kα radiation ($\lambda = 1.54$ Å) and a step size of 0.02°. Before, the analysis instrument was calibrated with lanthanum hexaboride (LaB_6).

Attenuated total reflectance Fourier transform infrared spectroscopy

Purified tyrosine reduced graphene oxide powder and graphene oxide were analyzed by using attenuated total reflectance Fourier transform infrared spectroscopy (JASCO ATR-FTIR 4100) to know the extent of deoxygenation. A control measurement of tyrosine has taken to know the surface functionalization of tyrosine reduced graphene oxide produced.

Raman analysis

The raman analysis for the as-synthesized graphene oxide and tyrosine reduced graphene oxide was carried out by using a Lab RAM HR visible single spectrometer outfitted with microscope and a Peltier-cooled CCD detector. Spectral measurements for the samples were taken at atmospheric conditions.

Atomic force microscopy

Multimode scanning probe microscope (NTMDTNTEGRA, Russia) was used for the atomic force microscopy analysis. Sample for analysis was prepared by coating a thin film of graphene onto p-type Si (100) substrates and dried, which was further kept under microscope for analysis.

Field emission scanning electron microscopy

Field emission scanning electron microscopy (FE-SEM) (SU-70, Hitachi instrument) was used for the field emission scanning electron microscopic analysis of the prepared graphene samples. Sample for analysis was prepared by coating the graphene dispersion onto the silicon wafer surface and allowed to dry under vacuum, which later used to take microscopic images.

Transmission electron microscopy

Transmission electron microscopy images at different magnifications were taken to know about the morphology of the prepared tyrosine reduced graphene oxide. JEOL-2100 F electron microscope was used at an operating voltage of 200 kV. A drop of aqueous dispersion of tyrosine reduced graphene oxide (0.5 mg mL^{-1}) prepared under ultrasonic conditions was placed on a copper grid and dried in vacuum, which was further placed under microscope to take the images.

Dynamic light scattering and zeta potential

Horiba Scientific Nanoparticci (SZ-100) instrument was used to know about the size distribution and surface charge of the formed tyrosine reduced graphene oxide sheets. Sample for analysis was prepared by dispersing tyrosine reduced graphene oxide in aqueous medium (0.5 mg mL^{-1}).

Results and discussion

Figure 1a has shown the UV–visible absorption spectra of graphene oxide, tyrosine reduced graphene oxide and tyrosine reduced graphene oxide (TRGO)/Ag. Spectrum of graphene oxide represents a peak at 230 nm, corresponding to the π–$\pi*$ transitions of the C=C bond and a shoulder peak at around 300 nm, which is ascribed to n–$\pi*$ transitions of the C=O groups (data not shown). During the reduction of graphene oxide by tyrosine, the peak at 230 nm is gradually red-shifted to $\sim$270 nm with reduction time, indicating the structural ordering with enriching of π-electron concentration, which reflects the restoration of sp^2 carbon. However, the spectrum of TRGO/Ag reflects peaks corresponding to both tyrosine reduced graphene oxide and surface plasmon resonance of silver nanoparticles, confirming the formation of composite.

The d-spacing values of tyrosine reduced graphene oxide and graphene oxide are the essential parameters to assess their structural information. The X-ray diffractogram of graphene oxide is compared with reduced graphene oxide synthesized by tyrosine (Fig. 1b). The peak at 2θ of 11.8° appeared in the X-ray diffractogram pattern of graphene oxide corresponds to the d-spacing of 0.7 nm, indicating the incorporation of oxygen functionalities between the layers of graphite after oxidation by modified Hummers method. The presence of these oxygen moieties causes an increase in the interlayer spacing and leads to the loose stacking of graphene oxide sheets. On the other hand, the X-ray crystallography pattern of reduced graphene oxide exhibits a weak diffraction peak at 2θ of 24.7°, characteristic to the d-spacing of 0.36 nm, indicating the restoration of the electronic structure of graphite after reduction with tyrosine. Also, the presence of diffraction peaks corresponding to silver nanoparticle in TRGO/Ag pattern indicated the formation of TRGO/Ag composite.

Further, X-ray photoelectron spectroscopy analysis was carried out to know about the reduction of graphene oxide and to determine oxidation state of silver decorated on the surface of tyrosine reduced graphene oxide (data not shown). The C1 s spectrum of tyrosine reduced graphene oxide represents the presence of main peak at 284.4 eV which corresponds to the C–C bond of sp^2 carbon in the graphitic structure, and other two peaks appeared at 286.4 and 288 eV are related to the C–O and C=O functionalities, respectively. The lower intensity of the C–O peak in tyrosine reduced graphene oxide compared to that of C–C peak indicates effective loss of oxygen functionalities after the reduction of graphene oxide. It is also found from X-ray photoelectron spectrum of silver at 3d core level that the Ag $3d_{3/2}$ and Ag $3d_{5/2}$ binding energies appear at 374.4 and 368.4 eV, respectively, confirming the decoration of silver nanoparticles onto the surface of tyrosine reduced graphene oxide (Saraschandra et al. 2016). From the X-ray photoelectron spectroscopy and X-ray diffraction results, it can be concluded the formation of silver nanoparticles on tyrosine reduced graphene oxide sheets.

Raman spectroscopy also gives the information about the structural changes in the graphene oxide after the reduction. From the Raman spectra of graphene oxide before and after reaction with tyrosine, it is found a higher intensity ratio of D to G band (I_D/I_G) is observed for graphene oxide after reduction by tyrosine (1.9) than before reduction (1.47), which indicates the effective reduction of graphene oxide and subsequent introduction of new defects in the structure of tyrosine reduced graphene oxide formed (Kuila et al. 2012). It is also found a shift in the G band of

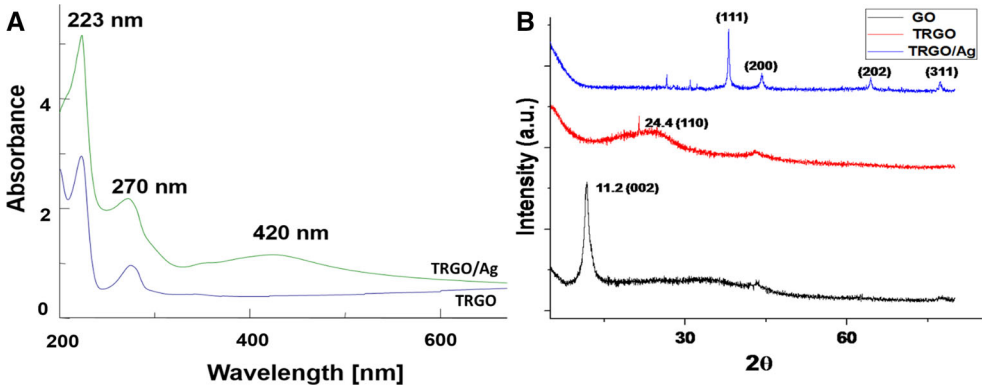

Fig. 1 **a** Comparative UV–visible spectral analysis for tyrosine reduced graphene oxide (TRGO) and tyrosine reduced graphene oxide/silver (TRGO/Ag) nanocomposite. Both the TRGO and TRGO/Ag composite showed absorbance peak of graphene at 270 nm. An extra surface plasmon resonance peak of silver nanoparticles is found at 420 nm in TRGO/Ag composite. **b** Comparative X-ray diffraction pattern for graphene oxide (GO), tyrosine reduced graphene oxide (TRGO) and tyrosine reduced graphene oxide/silver (TRGO/Ag) nanocomposite. There is a shift in the 2θ of GO from 11.2 to 24.4 of TRGO is observed. X-ray diffraction of TRGO/Ag showed the presence of diffraction peaks corresponding to silver nanoparticle at 38°, 46°, 64° and 77°

graphene oxide for about 10 cm^{-1} after reduction from 1598 to 1588 cm^{-1} signifying a high degree of deoxygenation by tyrosine (data not shown) (Li et al. 2013; Maddinedi et al. 2015a, b). All these results suggest an increase in the sp^2 domains after reduction.

The morphology of the synthesized tyrosine reduced graphene oxide was studied by FE-SEM analysis. The FE-SEM morphological images at different magnifications for tyrosine reduced graphene oxide are shown in Fig. 2a. From Fig. 2a, it was confirmed the presence of layered structures with transparent thin sheets. Additionally, tyrosine reduced graphene oxide sheets are quite well separated with large surface area.

The structure and morphology of tyrosine reduced graphene oxide, TRGO/Ag were studied via transmission electron microscopy. Figure 2b shows the transmission electron microscopy morphological images of the as-synthesized tyrosine reduced graphene oxide and TRGO/Ag composite, respectively. Transmission electron microscopy images have exhibited a transparent and silk-like sheet structure of tyrosine reduced graphene oxide (Fig. 2b). On the other hand, Fig. 2b also has shown the presence of a huge number of nanoparticles on the tyrosine reduced graphene oxide surface, indicating their decoration onto tyrosine reduced graphene oxide surface. The mean diameter of the silver nanoparticles is found to be 10 nm (calculated by using image J software).

Atomic force microscopy is an important tool to find the thickness of the tyrosine reduced graphene oxide samples (data not shown). From the atomic force microscopy, it is found the formation of thin sheet-like structures of graphene. The thickness of the obtained tyrosine reduced graphene oxide nanosheets is about 5.8 nm, indicating the formation of few layered graphene sheets.

The ATR-FTIR spectra of the native tyrosine, tyrosine reduced graphene oxide and graphene oxide are shown in Fig. 3. Spectrum of graphene oxide shows a broad O–H stretching vibrational band at 3100–3400 cm^{-1}. Additionally, the bands appeared at 1050, 1400 and 1618 cm^{-1} correspond to C–O stretch of carboxylic groups, tertiary alcohol and O–H bending and epoxide ring vibrations, successively. On the other hand, the spectrum of purified tyrosine reduced graphene oxide exhibits a significant reduction in the absorption band intensities of the oxygen moieties indicating the reduction of graphene oxide. Moreover, the tyrosine reduced graphene oxide also shows the vibrational bands of tyrosine at 1580, 1605 and 2927 cm^{-1} (broad band) which is characteristic of N–H bending vibrations, aromatic C=C and N–H stretching vibrations, respectively, indicating the capping of tyrosine onto the surface of tyrosine reduced graphene oxide. However, similar kind of results were observed with diastase-capped gold nanoparticles (Maddinedi et al. 2015a, b) and casein-stabilized reduced graphene oxide (Maddinedi et al. 2014), silver nanoparticles (Ashraf et al. 2013). On the other hand, the negative surface charge of graphene oxide dispersion was due to the existence of various oxygen functionalities, which became positive for reduced graphene oxide prepared by using polyallylamine (Kim and Min 2012). But the reduced graphene oxide prepared in the present synthetic method is stabilized by a number of tyrosine molecules, which is evidenced by its negative zeta potential of about −55 mV (data not shown). The net negative charge generated on the surface of tyrosine reduced graphene oxide after reduction may be due to the carboxylic groups of tyrosine residues present on the surface of graphene sheets, which is further responsible for preventing the aggregation of the successive tyrosine

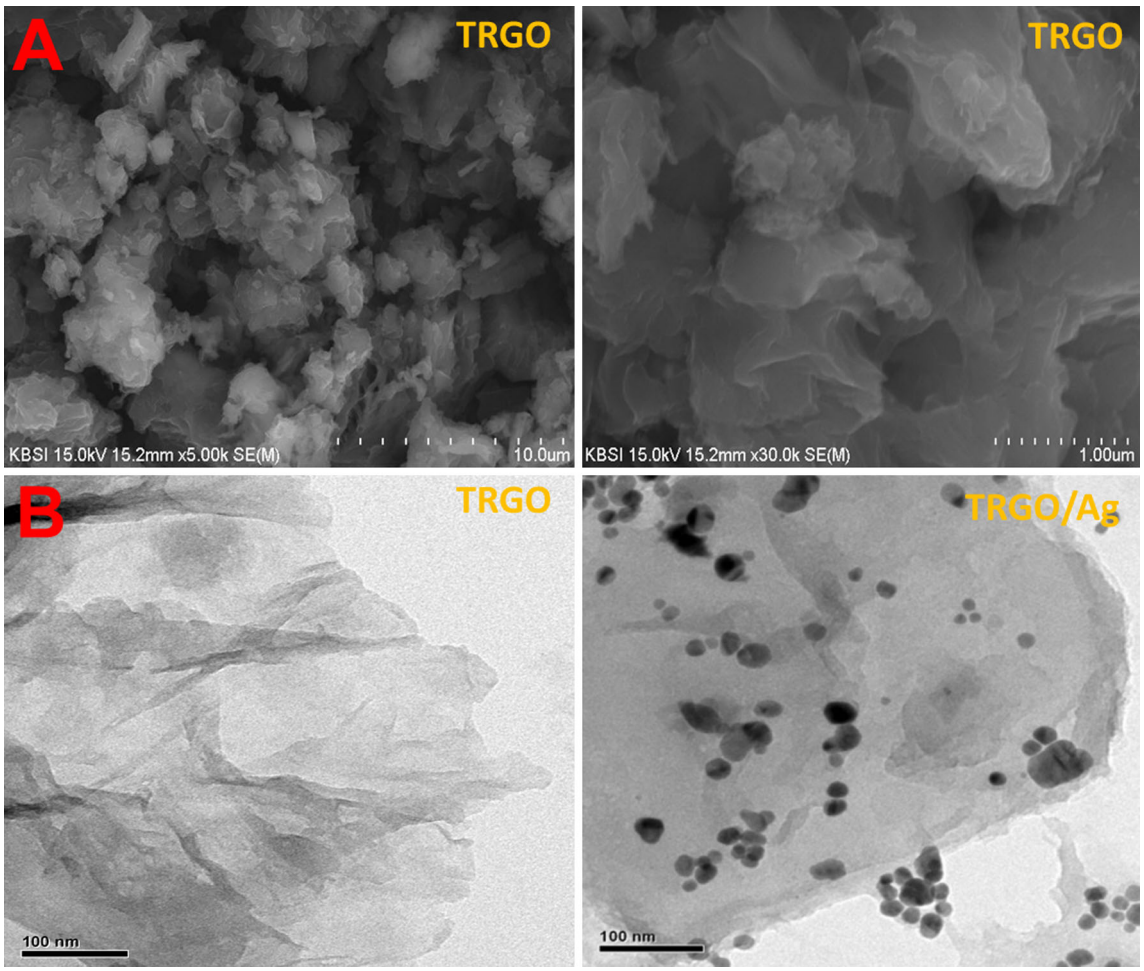

Fig. 2 **a** Field emission scanning electron microscopy (FE-SEM) images of tyrosine reduced graphene oxide (TRGO) at different magnifications showed the well-separated layered structures with transparent, thin graphene sheets possessing high surface area. **b** Transmission electron microscopy (TEM) images of tyrosine reduced graphene oxide (TRGO) and tyrosine reduced graphene oxide/silver composite (TRGO/Ag). Images showed the decoration of silver nanoparticles onto surface of transparent, silk-like graphene sheets

reduced graphene oxide sheets. All these results confirm the non-covalent adsorption of tyrosine molecules onto the tyrosine reduced graphene oxide surface.

Further, the size distribution of tyrosine reduced graphene oxide particles in aqueous medium was studied using dynamic light scattering by following a standard spherical model. Under prolonged sonication, the tyrosine reduced graphene oxide nanosheets were broken down into particles, and the mean particle size was found to be 412 nm (data not shown).

The plausible mechanism of graphene oxide reduction by tyrosine is explained as follows. From the literature, it is well known that the graphene oxide surface consists of various functional groups such as carbonyl, hydroxyl and epoxide (Thakur and Karak 2012). At pH 12, both the carbonyl and epoxide functionalities may be transformed into hydroxyl groups. The aromatic hydroxyl group of tyrosine may react with the hydroxyl groups present in graphene oxide via a SN_2 nucleophilic substitution mechanism resulting the elimination of two water molecules, which finally gives the tyrosine reduced graphene oxide (Maddinedi et al. 2015a, b). On the other hand, when tyrosine is added to the mixture of $AgNO_3$ and tyrosine reduced graphene oxide solution, the ionization of phenolic functionality of tyrosine takes place and transformed into its quinone form by electron transfer to Ag^+ ions, which later stabilizes the formed silver nuclei (Selvakannan et al. 2004). The silver nanoparticles that are formed after reduction will go and decorate onto the surface of the tyrosine reduced graphene oxide.

Catalytic activity

Further, to show the catalytic ability of the TRGO/Ag, the catalytic reduction of 4-nitrophenol (0.3 mM) with $NaBH_4$ (0.3 M) at room temperature in the presence of TRGO/Ag,

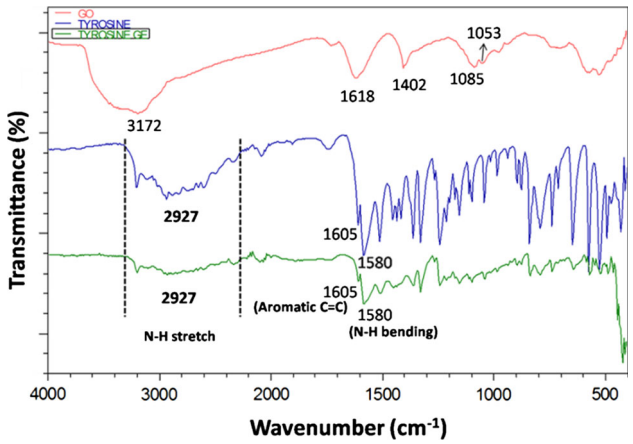

Fig. 3 Attenuated total reflectance Fourier transform infrared (ATR-FTIR) spectra of the native tyrosine, tyrosine reduced graphene oxide (tyrosine-GE) and graphene oxide (GO). The spectrum of tyrosine-GE exhibited a significant reduction in the absorption band intensities of the oxygen moieties found in GO (O–H and C–O). Also, spectra of tyrosine and tyrosine-GE showed common bands at 1580 cm^{-1} (N–H bending) and 2927 cm^{-1} (N–H stretching)

tyrosine reduced graphene oxide (0.025 mg/mL) was examined. A rapid decrease in the absorbance is at wavelength of 400 nm to zero within 5 min, in the presence of TRGO/Ag composite. However, no significant change in the absorbance was found in the presence of tyrosine reduced graphene oxide (data not shown). This has disclosed the no considerable catalytic ability of tyrosine reduced graphene oxide for the 4-nitrophenol reduction, while the TRGO/Ag possessed the good catalytic activity toward the 4-nitrophenol reduction and the observed catalytic activity is because of the silver nanoparticles decorated on the tyrosine reduced graphene oxide surface.

The effect of catalyst concentration on the catalytic reduction of 4-nitrophenol (0.3 mM) with $NaBH_4$ by different amounts of TRGO/Ag nanocomposites (0.025–0.1 mg/mL) is studied, where C_0 and C_t indicate the concentration of phenolate ion at zero time and at the time t, respectively. It was observed that the 4-nitrophenol reduction reaction followed the pseudo-first-order rate kinetics. The role of TRGO/Ag composite as catalyst for 4-nitrophenol reduction could be confirmed by the increase in the pseudo-first-order rate constant linearly with the increase in the catalyst concentration. It is also fascinating to note that the effects of 4-nitrophenol concentration (shown in Fig. 4a, b) and catalyst amount have shown to exhibit a linear relationship between ln (C_t/C_0) and time. However, these results are different from the previous reports which further suggested that the increase in catalytic activity was due to the synergistic effect of reduced graphene oxide used as the catalyst support.

The synergistic effect of the used tyrosine reduced graphene oxide might be explained as follows (Yeh and Chen 2014; Zhang et al. 2001). It is well known the conversion of 4-nitrophenol to 4-aminophenol might happen through two different routes: liquid phase and solid phase. During the reduction reaction, 4-nitrophenol could be adsorbed via π-π stacking interaction onto the tyrosine reduced graphene oxide surface due to its π-rich in nature as well as in bulk solution, and hence, a simultaneous decrease in the concentrations of 4-nitrophenol was observed. Due to these interactions, the availability of 4-nitrophenol near the silver nanoparticles on the tyrosine reduced graphene oxide surface increases, and hence, the contact between 4-nitrophenol and silver nanoparticles will be more efficient. The lower adsorption of 4-nitrophenol on the tyrosine reduced graphene oxide surface would result to the decreased 'k' value. On the other hand, there is a chance for the direct diffusion of 4-nitrophenol onto the silver nanoparticles surface from the bulk solution. Since, redox potential of smaller metal nanoparticles was higher, they could easily accelerate the electron transfer, and therefore, diffusion is slower than the heterogeneous charge transfer. In the previous reports, the catalysts and their supports used for the 4-nitrophenol reduction were exists in the form of nanoparticles (Hsu and Chen 2014), and therefore, the adsorption of 4-nitrophenol on their surface was not much prominent like that on the tyrosine reduced graphene oxide surface. Hence, the reaction occurred with a slower reaction rate, mainly through the collision of 4-nitrophenol molecules between the nanoparticles.

All these results demonstrated that the catalytic ability of TRGO/Ag catalyst used in this work was comparable or superior to the most of the previously used catalysts. Hence, the TRGO/Ag synthesized in the present work could be used as an efficient catalyst for the 4-nitrophenol reduction with $NaBH_4$.

Conclusion

We have shown the reduction of graphene oxide by tyrosine resulting in the formation of a suitable and efficient support for the preparation of graphene hybrids. ATR-FTIR and Zeta potential data revealed the adsorption of tyrosine molecules onto the reduced graphene oxide surface. Further, the synergistic effect of RGO/Ag nanocomposites for the catalytic reduction of 4-NP with $NaBH_4$ is shown via both the liquid-phase and solid-phase routes. Additionally, the presence of tyrosine onto the reduced graphene oxide surface is interesting for the biology-oriented applications. The present synthetic route provides a simple, green and low-cost alternative for the traditionally available chemical methods for the production of reduced graphene oxide and its hybrid materials.

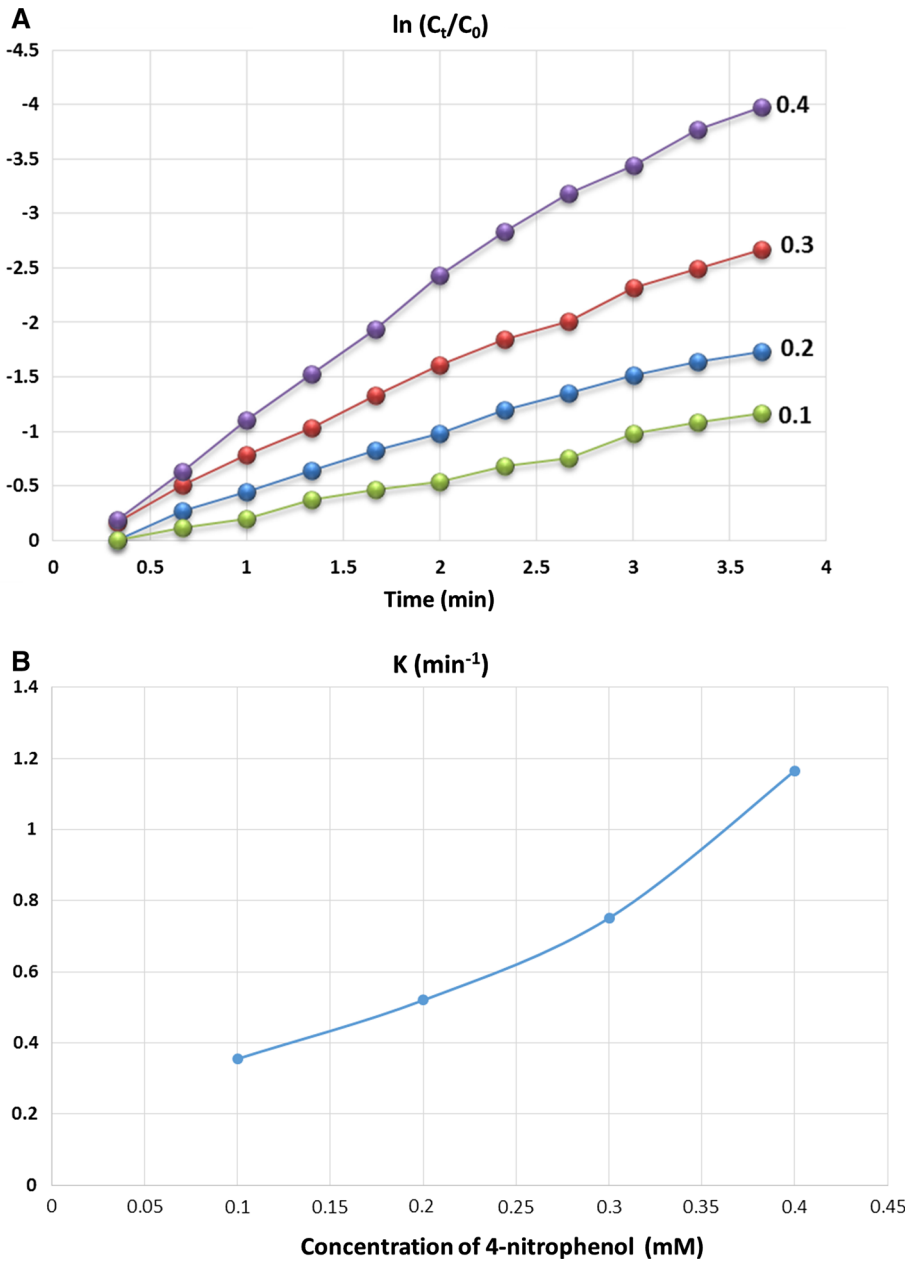

Fig. 4 **a** Plots of ln (C_t/C_0) versus time for the catalytic reduction of 4-nitrophenol with $NaBH_4$ by tyrosine reduced graphene oxide/silver nanocomposite at different concentration of 4-nitrophenol. **c** Plots showing the relationship between the pseudo-first-order rate constant versus concentration of 4-nitrophenol. An increase in the pseudo-first-order rate constant linearly with the increase in the catalyst concentration and catalyst

Acknowledgements Mr. SBM greatly acknowledges the help of VIT University, Vellore-632014, India for the financial help and platform given to do this research. Also, SBM acknowledges the help from Korean Basic Science Institute, Busan Center, Busan 618 230, South Korea for Transmission electron microscopy, X-ray photoelectron spectroscopy and FE-SEM facilities.

References

Akhavan O, Ghaderi E (2012) Escherichia coli bacteria reduce graphene oxide to bactericidal graphene in a self-limiting manner. Carbon 50:1853–1860. doi:10.1016/j.carbon.2011.12.035

Ashraf S, Abbasi AZ, Pfeiffer C, Hussain SZ, Khalid ZM, Gil PR, Parak WJ, Hussain I (2013) Protein-mediated synthesis, pH-induced reversible agglomeration, toxicity and cellular interaction of silver nanoparticles. Colloids Surf B 102:511–518. doi:10.1016/j.colsurfb.2012.09.032

Chai L, Wang T, Zhang L, Wang H, Yang W, Dai S, Meng Y, Li X (2014) A Cu–m-phenylenediamine complex induced route to fabricate poly(m-phenylenediamine)/reduced graphene oxide hydrogel and its adsorption application. Carbon 81:748–757. doi:10.1016/j.carbon.2014.10.018

Geim AK, Novoselov KS (2007) The rise of graphene. Nat Mater 6:183–191. doi:10.1038/nmat1849

Hsu KC, Chen DH (2014) Green synthesis and synergistic catalytic effect of Ag/reduced grapheme oxide nanocomposites. Nanoscale Res Lett 9:1–10. doi:10.1186/1556-276X-9-484

Kim YK, Min DH (2012) Simultaneous reduction and functionalization of graphene oxide by polyallylamine for nanocomposite formation. Carbon Lett 13:29–33. doi:10.5714/CL.2012.13.1.029

Kuila T, Bose S, Khanra P, Mishra AK, Kim NH, Lee JH (2012) A green approach for the reduction of graphene oxide by wild carrot root. Carbon 50:914–921. doi:10.1016/j.carbon.2011.09.053

Li J, Xiao G, Chen C, Li R, Yan D (2013) Superior dispersions of reduced graphene oxide synthesized by using gallic acid as reductant and stabilizer. J Mater Chem 1:1481–1487. doi:10.1039/C2TA00638C

Maddinedi SB, Mandal BK (2014) Low-cost and eco-friendly green methods for graphene synthesis. Int J Nano Sci Technol 3:46–61

Maddinedi SB, Mandal BK (2015) Biofabrication of reduced graphene oxide nanosheets using terminalia bellirica fruit extract. Curr nanosci. 12:94–102. doi:10.2174/1573413711666150520224358

Maddinedi SB, Mandal BK, Vankayala R, Kalluru P, Tammina SK, Kiran Kumar HA (2014) Casein mediated green synthesis and decoration of reduced graphene oxide. Spectrochim. Acta Part A Mol Biomol Spectrosc 126:227–231. doi:10.1016/j.saa.2014.01.114

Maddinedi SB, Mandal BK, Ranjan S, Dasgupta N (2015a) Diastase assisted green synthesis of size controllable gold nanoparticles. RSC Adv 5:26727–26733. doi:10.1039/C5RA03117F

Maddinedi SB, Mandal BK, Vankayala R, Kalluru P, Pamanji SR (2015b) Bioinspired reduced graphene oxide nanosheets using Terminalia chebula seeds extract. Spectrochim Acta Part A 145:117–124. doi:10.1016/j.saa.2015.02.037

Maddinedi SB, Mandal BK, Patil SH, Andhalkar VV, Ranjan S, Dasgupta N (2017) Diastase induced green synthesis of bilayered reduced graphene oxide and its decoration with gold nanoparticles. J Photochem Photobiol B 166:252–258. doi:10.1016/j.jphotobiol.2016.12.008

Paredes JI, Rodil SV, Merino MJF, Guardia L, Alonso AM, Tascon JMD (2011) Environmentally friendly approaches toward the mass production of processable graphene from graphite oxide. J Mater Chem 21:298–306. doi:10.1039/C0JM01717E

Perera SD, Mariano RG, Nijem N, Chabal Y, Ferraris JP, Balkus KJ (2012) Alkaline deoxygenated graphene oxide for supercapacitor applications: an effective green alternative for chemically reduced graphene. J Power Sources 215:1–10. doi:10.1016/j.jpowsour.2012.04.059

Saraschandra N, Lakshmi Kumari P, Das RK, Sivakumar A, Patil SH, Andhalkar VV (2016) Amelioration of excision wounds by topical application of green synthesized, formulated silver and gold nanoparticles in albino Wistar rats. Mater Sci Eng C 62:293–300. doi:10.1016/j.msec.2016.01.069

Selvakannan PR, Swami A, Srisathiyanarayanan D, Shirude PS, Pasricha R, Mandale AB, Murali S (2004) Synthesis of aqueous Au core-Ag shell nanoparticles using tyrosine as a pH-dependent reducing agent and assembling phase-transferred silver nanoparticles at the air-water interface. Langmuir 20:7825. doi:10.1021/la049258j

Si Y, Samulski ET, Hill C, Carolina N (2008) Synthesis of water soluble graphene. Nano Lett 8:1679–1682. doi:10.1021/nl080604h

Stankovich S, Dikin DA, Piner RD, Kohlhaas KA, Kleinhammes A, Jia Y (2007) Synthesis of graphene-based nanosheets via chemical reduction of exfoliated graphite oxide. Carbon 45:1558–1565. doi:10.1016/j.carbon.2007.02.034

Thakur S, Karak N (2012) Green reduction of graphene oxide by aqueous phytoextracts. Carbon 50:5331–5339. doi:10.1016/j.carbon.2012.07.023

Wang G, Yang J, Park J, Gou X, Wang B, Liu H, Yao J (2008) Facile synthesis and characterization of graphene nanosheets. J Phys Chem C 112:8192–8195. doi:10.1021/jp710931h

Yeh CC, Chen DH (2014) Ni/reduced graphene oxide nanocomposite as a magnetically recoverable catalyst with near infrared photothermally enhanced activity. Appl Catal B Environ 150–151:298–304. doi:10.1016/j.apcatb.2013.12.040

Zhang YW, Liu S, Lu WB, Wang L, Tian JQ, Sun XP (2001) In situ green synthesis of Au nanostructures on graphene oxide and their application for catalytic reduction of 4-nitrophenol. Catal Sci Technol 1:1142–1144. doi:10.1039/C1CY00205H

Zhang L, Chai L, Duan J, Li G, Wang H, Yu W, Sang P (2011) One-step and cost-effective synthesis of micrometer-sized saw-like silver nanosheets by oil/water interfacial method. Mater Lett 65:1295–1298. doi:10.1016/j.matlet.2011.01.062

Zhang L, Wang T, Wang H, Meng Y, Yu W, Chai L (2013) Graphene@poly (m phenylenediamine) hydrogel fabricated by a facile post-synthesis assembly strategy. Chem Commun 49:9974–9976. doi:10.1039/C3CC45261A